Computational Materials Science 65 (2012) 197–202

Contents lists available at SciVerse ScienceDirect

Computational Materials Science

journal homepage: www.elsevier.com/locate/commatsci

FEM modeling of the flow curves and failure modes of dual phase steels with different martensite volume fractions using actual microstructure as the representative volume

M. Marvi-Mashhadi, M. Mazinani, A. Rezaee-Bazzaz *

Department of Metallurgy and Materials Engineering, Faculty of Engineering, Ferdowsi University of Mashhad, Mashhad, Iran

A R T I C L E I N F O

Article history:
Received 29 April 2012
Received in revised form 6 June 2012
Accepted 8 July 2012

Keywords:
Finite element method (FEM)
Mechanical characterization
Steel
Failure

A B S T R A C T

The flow curves and failure modes of dual phase steels containing 18 and 44 vol.% martensite were predicted using a micromechanical-based finite element method. Actual microstructures of the dual phase steels obtained by scanning electron microscope (SEM) were used as the representative volume elements (RVEs) in the calculations. Ductile failure of the representative volume was predicted as plastic strain localization during deformation. Computations were conducted on the representative volume to quantitatively evaluate the effects of mechanical properties of the dual phase constituents and their volume fractions on the macroscopic mechanical properties of the dual phase steels. The computational results were compared with the experimentally obtained data. It was found that the computational method can predict well both strength and ductility of the studied dual phase steels. Moreover, based on the computational results, shear dominant failure mode occurs in both of the studied dual phase steels which correlate with experimental findings.

1. Introduction

Dual phase steels having a microstructure consisting of hard martensite islands within a ferrite matrix have received considerable attention due to their high tensile to yield strength ratio, continuous yielding behavior, high work hardening rate and good ductility. These favorable mechanical properties of dual phase steels result in a weight reduction at a reasonable strength level and superior formability compared with the high strength low alloy (HSLA) steels [1–3]. It has been reported that macroscopic mechanical behavior of dual phase steels depends on various factors, such as, the grain size of the ferrite and the volume fraction, morphology and carbon content of the martensite phase [3–7]. The strength of the ferrite phase is mainly controlled by the steel chemistry, grain size and initial dislocation density, while the strength of martensite depends primarily on its carbon content and to a lesser extent, on its morphology [8,9].

There are several reports about predicting the evolution of deformation behavior and failure mechanism of multi-phase steels from their microstructures by analytical and numerical methods. These reports include the regression method according to the chemical composition of steels [10], the secant method using Eshelby's model [3,11] and the finite element method (FEM) [1,2,12–16]. Among these modeling approaches, FEM has the advantage of taking into account the morphologies of phases as close to the actual microstructures as possible. The majority of these studies attempt to predict and quantify work hardening behavior of multi-phase steels while remain their ultimate tensile strength, ultimate ductility and failure modes unpredicted. The microstructure of multi-phase steels has been simulated using some simplified models such as the stacked hexagon array model [1,2,12–16], and the Voroni cell model [17] in most of these investigations. In a few recent papers, the actual microstructure of multi-phase steels has been used as the representative volume element in the finite element calculations [15,18–21]. In these papers, work hardening behavior as well as ultimate tensile strength, ultimate ductility and failure modes of multi-phase steels have been estimated fairly well.

It is generally accepted that ductile fracture strongly depends on the microstructure, voids, inclusions and microcracks in the material [22]. Ductile materials typically exhibit localized deformation before final fracture and many multi-scale models have been proposed in such materials [23–25]. Some material instability theories in computational plasticity have been used and constitutive bifurcation criteria as indicators of the initiation of plastic localization have been developed [26–29]. In prediction of ductility using the finite element methods, in which actual microstructure of multi-phase steels used as a representative volume, no prescribed failure criterion needs to be used and ductile failure is predicted as the natural outcome of the plastic strain localization due to the incompatible deformation between the hard and soft

* Corresponding author. Tel.: +98 5118763305.
E-mail address: bazaz-r@um.ac.ir (A. Rezaee-Bazzaz).

0927-0256/$ - see front matter © 2012 Elsevier B.V. All rights reserved.
http://dx.doi.org/10.1016/j.commatsci.2012.07.032

Table 1
Chemical composition of the steel used as the starting material.

Element	C	Mn	Si	Mo	Ti	Nb	V	Cr	Ni	Cu	P	S	Al
Wt.%	0.06	2.0	0.07	0.15	0.014	0.002	0.004	0.04	0.015	0.01	0.012	0.002	0.037

Table 2
Summary of the processing conditions, and the resulting martensite volume fractions.

Heating rate (°C/S)	*T* (°C)	Holding time (s)	Martensite volume fraction (%)
1	755	60	18
1	820	60	44

phases. To the authors' knowledge, none of the other modeling approaches for predicting the ductility of multiphase steels have such an exceptionally good characteristic, which causes the application of this method to be general and very simple.

The aim of this work is to predict the flow curves and ductility of dual phase steels containing 18 and 44 vol.% of martensite using the finite element method, in which the actual microstructure of the steels were used as the representative volume elements. In all other similar works reported in the literature, the mechanical properties of constituent phases of the multi-phase steels have been determined using in situ high energy X-ray diffraction experiments while in the present study, the mechanical properties of these phases have been estimated based on the experimental results reported in the literature [12,30].

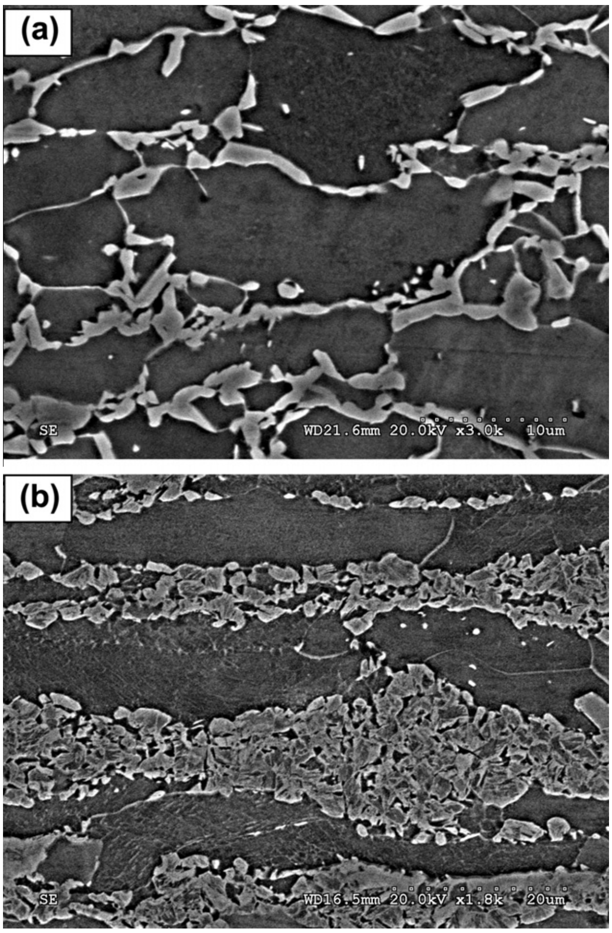

Fig. 1. Actual microstructure of the studied dual phase steels, (a) dual phase steel containing 18 vol.% martensite, (b) dual phase steel with 44 vol.% martensite.

2. Experimental procedure

A cold rolled low carbon steel (DP600 steel supplied by Stelco. Inc., Hamilton ON) with an initial microstructure of ferrite plus 8–10% pearlite was used as the starting material to produce dual phase microstructures. The chemical composition of this steel is given in Table 1. Samples of the starting material were heated to various intercritical temperatures and then quenched with a water/helium gas mixture. Steel samples for optical metallography were polished following a detailed procedure recommended by Buehler Ltd. [30]. The polished samples were etched in a solution prepared by adding 10 g sodium metabisulfide into 100 mL water. The quantitative measurements were conducted using Clemex image analysis software. Average martensite volume fraction was determined using 20–30 images taken from different locations in the sample. Table 2 summarizes the various combinations of heating rate, intercritical annealing temperatures and holding times, together with the resultant martensite volume fractions. Tensile tests were conducted using an MTS universal tensile testing machine at a strain rate of $2 \times 10^{-3}\ s^{-1}$ using sub size tensile specimens having the gage length of 20 mm.

3. Finite element analysis

Theoretically, the macroscopic behavior of dual phase steels can be modeled from the individual atoms, crystal structure, grain structure and microstructure up to the macroscopic constitutive level. Even though phenomenological constitutive modeling is the most computationally efficient, it usually provides no information about ductility and failure mode of the materials [15]. In this study, the mechanical behavior of each of the constituent phases of the studied steels have been considered to be isotropic and homogeneous to simulate the macroscopic mechanical behavior, ductility and failure modes of the studied steels in a computationally efficient manner. Moreover, the grain structure of the two phases have been explicitly modeled without consideration of the grain boundary decohesion, the same as that used by Choi et al. [15].

Fig. 1a and b shows actual microstructures captured by the scanning electron microscope (SEM) from the mid plane along the loading direction of the tensile specimens of the dual phase steels containing 18 and 44 martensite volume fractions, respectively. The black and white areas in these microstructures represent the ferrite and martensite phases, respectively. These figures were used for subsequent image processing and importing to the ABAQUS general purpose commercial finite element code [31]. It is worth noting that in the micrographs taken for considering the representative volume elements, the morphology and volume fractions of the constituent phases should be the same as the mean phase volume fraction and morphologies of the studied materials. After importing the SEM numerical image processed micrographs into ABAQUS, these micrographs were discretized so as the phase boundaries model explicitly with finer meshes for subsequent investigations of failure initiation. Two dimensional three-node plane stress elements (CPS3) were used in this study for discretization. Since tensile specimens have been machined from the dual phase steel sheets and because these specimens undergo in plane loading during uniaxial tensile tests, application of plane stress elements for discretization seems to be rational. The resulting discretized actual microstructures of the two studied dual phase steels have been shown in Fig. 2a and b.

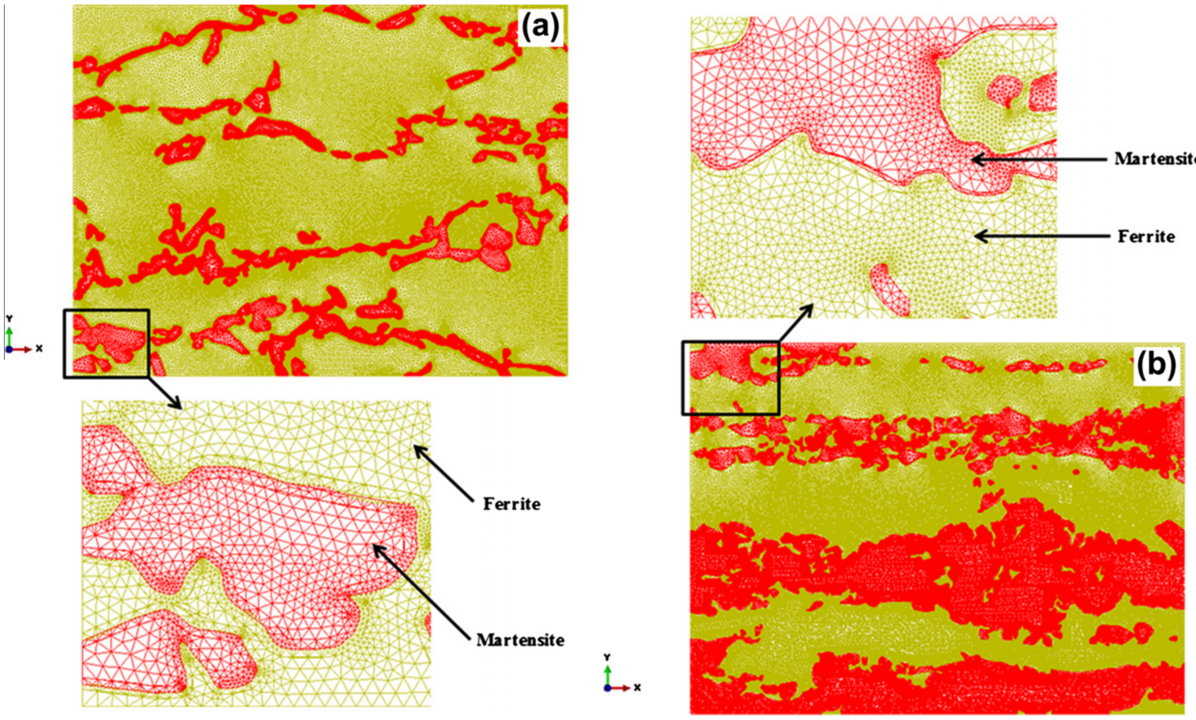

Fig. 2. Finite element model used for, (a) dual phase steels containing 18 vol.% of martensite, (b) dual phase steel with 44 vol.% of martensite.

Table 3
Voce equation constants for ferrite and martensite having 0.31%, 0.13% carbon content.

Phase	*A* (MPa)	*B* (MPa)	*C*
Ferrite	624.246	301.358	10.398
Martensite with 0.31% carbon	2022.704	2113.316	127.9604
Martensite with 0.13% carbon	1300	360	13

For modeling the uniaxial tensile loading, the same displacement was applied on the nodes located along the right edge of each of the representative volume elements in the *x* direction while these nodes can move freely in the *y* direction and the nodes located in the left edges of the representative volume elements were considered not to move in the *x* direction but allowed to move freely in the *y* direction. Since the representative elements should remain rectangular during deformation, the top and bottom edges of the elements were constrained so that all the nodes located along these edges displace the same in the *y* direction. Macroscopic engineering stress was calculated by dividing the reaction force of the right edge of the volume element in the *x* direction by initial length and macroscopic engineering strain in the *x* direction was obtained by dividing the right edge displacement of the volume element by the initial length of the horizontal edge of the volume element.

In this study, each of the constituent phases of the dual phase steels has been considered to be an elastic–plastic solid with $E = 210$ GPa and $\nu = 0.3$ [1–3]. The Voce equation was adopted for predicting the stress–strain curves of both ferrite and martensite phases. The constants of Voce equation, i.e. Eq. (1), were obtained by nonlinear least square method.

$$\sigma = A - B\exp(-C\varepsilon) \tag{1}$$

Since austenite to martensite transformation is diffusionless, it is reasonable to assume that the carbon content of martensite phase at room temperature to be the same as that in the austenite phase at the intercritical temperature. Therefore, using equilibrium Fe–C phase diagram and the temperature at which each of the studied steels has been intercritically annealed, the carbon content of martensite in dual phase steels containing 18 and 44 vol.% of martensite has been estimated to be 0.31 and 0.13, respectively. The experimental data reported in the previous researches were used for obtaining the Voce constants [12,30]. These constants have been shown in Table 3. Fig. 3 shows the stress–strain curves for the ferrite and martensite having 0.31 and 0.13 carbon content, together with predicted stress–strain curves obtained by the Voce equation. As these curves show, there is a good agreement between experimental and calculated flow curves in the plastic region.

4. Results and discussion

Fig. 4a and b shows the engineering stress–engineering strain curves predicted by the numerical method based on the considered representative volume elements, together with the experimental data obtained by uniaxial tensile test for the dual phase steels containing 18 and 44 vol.% of martensite, respectively. As these curves show, there is a good agreement between experimental and predicted results. Specifically, the employed numerical method is capable of estimating the UTS, the engineering strain corresponding to the UTS and the engineering failure strain fairly well. Comparing the results of the present study with those reported in the literature about using the same numerical method for modeling multi-phase steels, it is clear that although the mechanical behavior of the constituent phases used in the current work has not been obtained by in situ techniques, the predicted engineering stress–engineering strain curves in this study have similar accuracy with those reported in the literature.

Fig. 5a–d shows the equivalent plastic strain distribution in the considered representative volume element at different engineering strains for the dual phase steel containing 18 vol.% of martensite. As mentioned before, in the modeling procedure used in the current study, ductile failure is simulated as the plastic strain localiza-

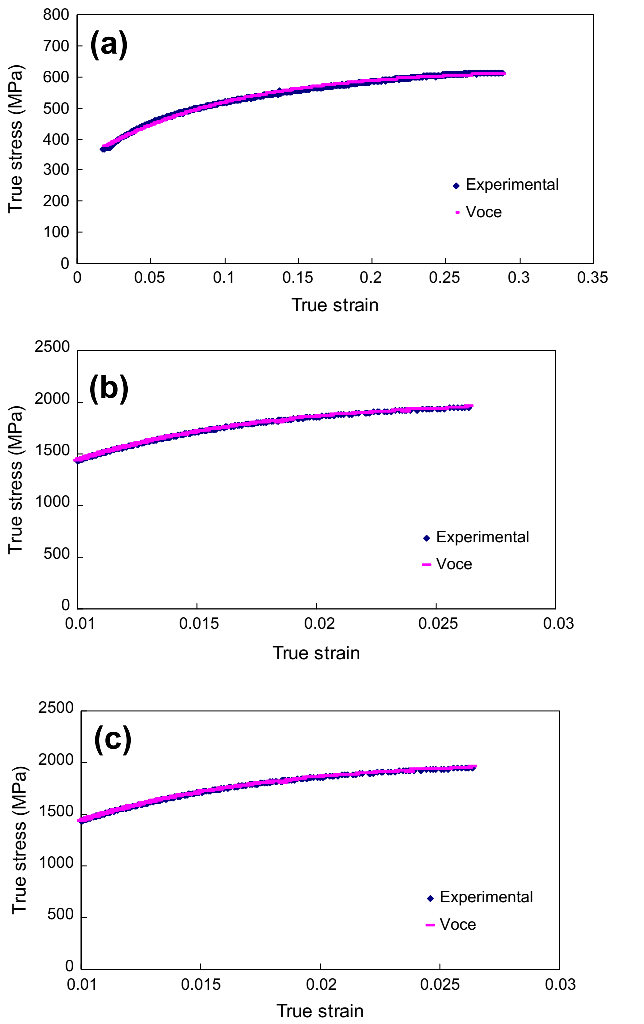

Fig. 3. Experimental stress–strain curves together with predicted ones using Voce equation, (a) ferrite, (b) martensite having 0.13% carbon content and (c) martensite having 0.31% carbon content.

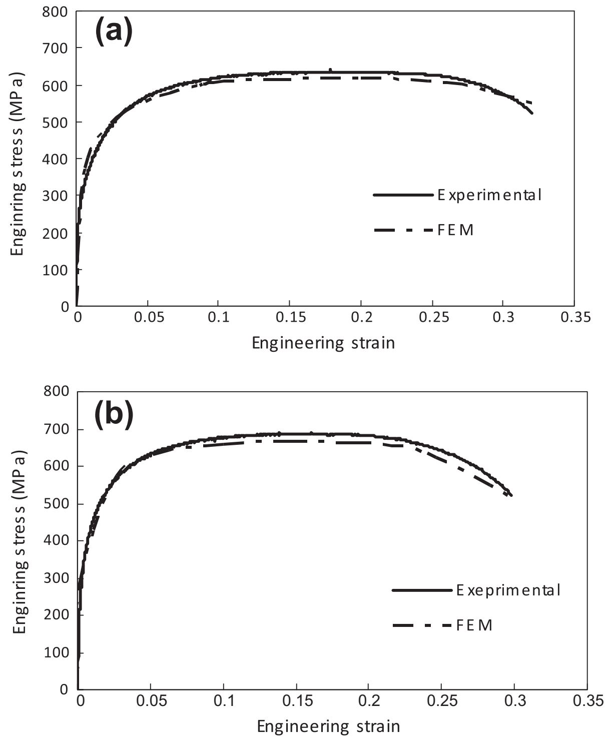

Fig. 4. Engineering stress–engineering strain curves of the studied dual phase steels, (a) dual phase steel containing 18% martensite volume fraction, (b) dual phase steel with 44% martensite volume fraction.

tion. According to the results illustrated in Fig. 5, plastic strain localization first appears in the element and propagates along the inclined direction with respect to the loading direction. Another strain localization appears at a different position by increasing the load and then propagates in the same manner as before. Finally, failure of the representative volume element is caused by the growth and coalescence of these initial strain localizations. Therefore, it can be said that the failure mode of the dual phase steel containing 18 vol.% of martensite is shear dominant [15].

Fig. 6a–d illustrates the sequence of equivalent plastic strain localization during loading of the considered representative volume element for the dual phase steel containing 44 vol.% of martensite. The initiation and the relative orientation of the plastic strain localization in these figures show that the failure mode of the dual phase steel containing 44 vol.% of martensite is also shear dominant. A comparison of Figs. 5 and 6 show that in the dual phase steel containing 44 vol.% of martensite plastic deformation takes place in the martensite phase while in the dual phase steel with 18% martensite volume fraction the martensite phase deforms elastically which correlates with experimental findings reported in the literature [3].

The optical pictures of the tensile specimens of dual phase steels containing 18 and 44 vol.% of martensite after failure are depicted in Fig. 7a and b, respectively. In these pictures the loading

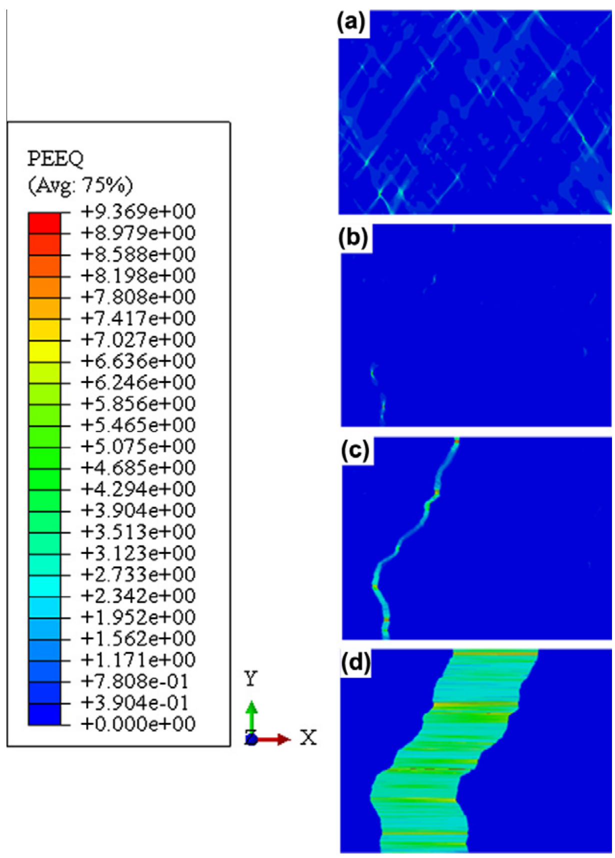

Fig. 5. Distribution of equivalent plastic strain for dual phase steel containing 18 vol.% of martensite at various average strain levels of (a) 3%, (b) 10%, (c) 21% and (d) 31%.

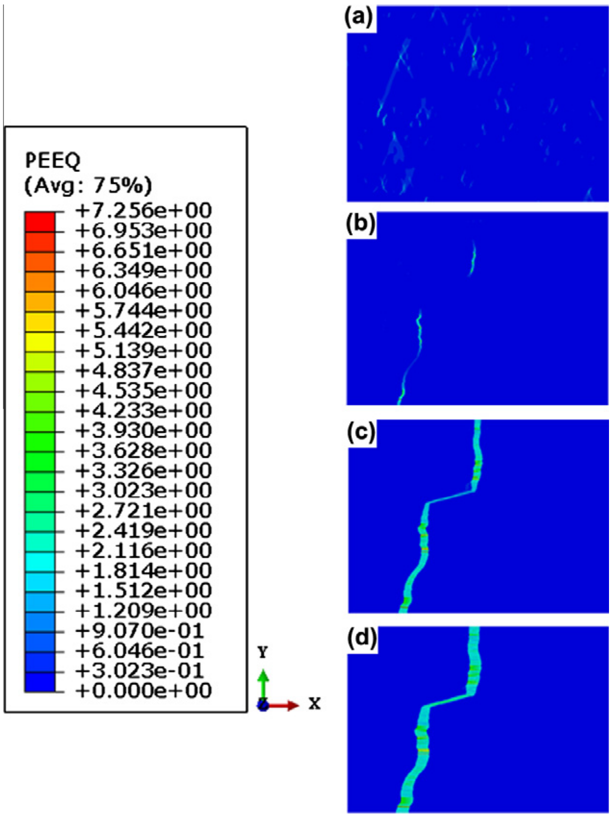

Fig. 6. Distribution of equivalent plastic strain for dual phase steel containing 44 vol.% of martensite at various average strain levels of (a) 3.5%, (b) 10%, (c) 20% and (d) 28%.

directions are the same as those of corresponding representative volume elements used in the numerical calculations. Comparing the shape and the relative orientation of the fractured region with those predicted by numerical method shown in Fig. 5b and 6b, it can be said that the predicted failure modes of the studied dual phase steels are almost the same as those obtained by the experiments.

As can be observed in Fig. 4, the engineering failure strain of the dual phase steel with 18% martensite volume fraction is almost the same as that of the steel having 44 martensite volume percent even though their martensite volume fraction is different Choi et al. investigated the influence of martensite initial yield stress, hardening rate and volume fraction on engineering failure strain [15]. Based on their investigation, increasing both initial yield strength and volume fraction of martensite results in a decrease in failure strain. Reviewing the results reported in this study shows that it is possible that two dual phase steels with different martensite volume fractions have the same failure strain but with different initial martensite yield strength. Reminding that the martensite phase in the dual phase steel containing 18 martensite volume fraction has higher yield strength than that of the martensite phase in the dual phase steel with 44 martensite volume fraction, it can be said that increasing failure strain in the dual phase steel with 44 martensite volume fraction because of decreasing the martensite yield strength compensates for decreasing failure strain caused by increasing martensite volume fraction, when engineering failure strain of dual phase steel containing 44 vol.% of martensite compare with that of dual phase steel with 18% martensite volume fraction. Based on this reasoning, the cause of similarity of engineering failure strains and failure modes in the two studied dual phase steels can be described.

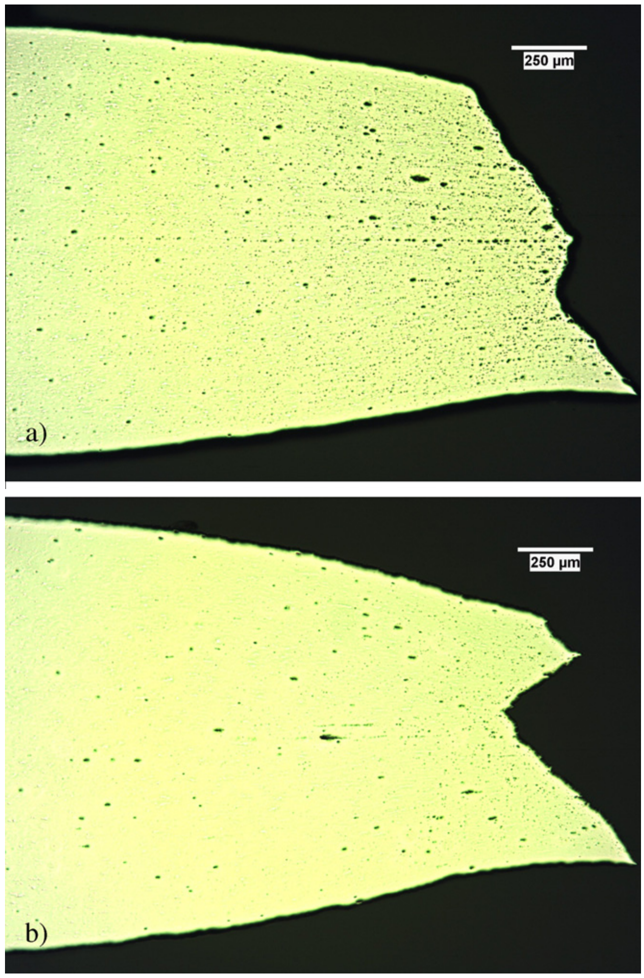

Fig. 7. Optical micrographs of failed tensile specimens of dual phase steels with (a) 18% martensite volume fraction and (b) 44% martensite volume fraction.

5. Conclusion

In this study, finite element modeling based on the actual microstructure has been used to predict engineering stress–engineering strain curves of dual phase steels containing 18 and 44 vol.% of martensite. The mechanical properties of each of the constituent phases obtained from tensile tests performed on fully ferritic and fully martensitic steels have been used in the numerical study. No prescribed failure criterion has been considered for the two constituent phases and failure predicted as the natural outcome of plastic localization caused by incompatible deformation between hard and soft phases in the representative volume elements. The results indicate that there is a good agreement between experimental and simulated engineering stress–engineering strain curves, although the mechanical behavior of the constituent phases has not been obtained by in situ methods. The results of the present study also show that the utilized numerical method is able to estimate failure engineering strain of the studied dual phase steels in a reasonable manner. Moreover, it has been found that shear dominant failure mode can be proposed for the two studied dual phase steels, which correlates well with experimental findings.

Acknowledgement

The Authors wish to thank Prof. W.J. Poole at the University of British Columbia for providing the steel for this investigation.

References

[1] F.M. Al-Abbasi, J.A. Nemes, Int. J. Mech. Sci. 45 (2003) 1449–1465.
[2] F.M. Al-Abbasi, J.A. Nemes, Int. J. Solid Struct. 40 (2003) 3379–3391.
[3] M. Mazinani, W.J. Poole, Metall. Mater. Trans. A 38 (2007) 328–339.
[4] N.J. Kim, A.H. Nakagawa, Mater. Sci. Eng. 83 (1986) 145–149.
[5] M. Erdogan, J. Mater. Sci. 37 (2002) 3623–3630.
[6] S. Sun, M. Pugh, Mater. Sci. Eng. A 335 (2002) 298–308.
[7] K.S. Park, K.T. Park, D.L. Lee, C.S. Lee, Mater. Sci. Eng. A 449–451 (2007) 1135–1138.
[8] F.B. Pickering, Constitution and properties of steels, Weinheim, Germany, 1992.
[9] W.C. Leslie, The Physical Metallurgy of Steels, Mc Graw-Hill, New York, 1981.
[10] T. Gladman, I.D. Mc Ivor, F.B. Pickering, J. Iron. Steel. Inst. 210 (1972) 916–930.
[11] .Y. Tomato, T. Ohnuki, M. Umemoto, Proc. 15th Int. Symp. Mater. Sci. Roskilde (1994) 595–600.
[12] .T. Huper, S. Endo, N. Ishikawa, K. Osawa, ISIJ Int. 30 (1999) 288–294.
[13] D.W. Shu, J.H. Bae, J.Y. Cho, K.H. Oh, H.C. Lee, ISIJ Int. 41 (2001) 782–787.
[14] H. Koushyar, B. Tavakol, V. Madhavan, Micromechanical modeling of ferrite/pearlite steels, in: Proceedings of the 4th Annual GRASP Symposium, Wichita State University, 2008, pp. 45–46.
[15] K.S. Choi, W.N. Liu, X. Sun, M.A. Khaleel, Metall. Mater. Trans. A 40 (2009) 796–809.
[16] M. Marvi-Mashhadi, A. Rezaee-Bazzaz, M. Mazinani, Mater. Sci. Forum. 706–709 (2012) 1503–1508.
[17] M. Nygards, P. Gudmundson, Mater. Sci. Eng. A 325 (2002) 435–443.
[18] X. Sun, K.S. Choi, W.N. Liu, M.A. Khaleel, Int. J. Plast. 25 (2009) 1888–1909.
[19] A. Soulami, K.S. Choi, W.N. Liu, X. Sun, M.A. Khaleel, Y. Ren, Y.D. Wang, Metall. Mater. Trans. A 41 (2010) 1261–1268.
[20] K.S. Choi, W.N. Liu, X. Sun, M.A. Khaleel, Y. Ren, Y.D. Wang, Metall. Mater. Trans. A 39 (2008) 3089–3096.
[21] K.S. Choi, A. Soulami, W.N. Liu, X. Sun, M.A. Khaleel, Comput. Mater. Sci. 50 (2010) 720–730.
[22] F.A. Mc Clintock, J. Appl. Mech. 35 (1968) 363–371.
[23] Y. Wei, G. Xu, Int. J. Plast. 21 (2005) 2123–2149.
[24] N. Bonora, A. Ruggiero, L. Epsito, D. Gentile, Int. J. Plast. 22 (2006) 2015–2047.
[25] P.J. Sanchez, A.E. Huespe, J. Oliver, Int. J. Plast. 24 (2008) 1008–1038.
[26] J.P. Miles, J. Mech. Phys. Solids 19 (1971) 89–102.
[27] A. Needleman, J. Mech. Phys. Solids 20 (1972) 111–127.
[28] S. Storen, J.R. Rice, J. Mech. Phys. Solids 23 (1975) 421–441.
[29] Y. Li, D. Karr, Int. J. Plast. 25 (2009) 1128–1153.
[30] M. Mazinani, PhD thesis, The University of British Columbia, Vancouver, BC 2006.
[31] ABAQUS General Purpose Finite Element Program, Version 6.10-1 Dassault Systèmes Simulia Corp., Providence, RI, USA, 2010.